The Robustness and Design of Constrained Cross-directional Control via Integral Quadratic Constraints

R. M. Morales, *Member, IEEE,* and W. P. Heath, *Member, IEEE,*

***Abstract*—A robust stability test for a class of constrained cross-directional controllers is found. Under special circumstances, the stability test is executed on a mode-by-mode basis and greatly simplified to a frequency-domain criterion. The test is also exploited to develop tuning algorithms. The control system involves a quadratic program embedded within an internal model control anti-windup structure and achieves optimal steady-state performance when the plant is known. Both the nonlinearity in the controller and the plant uncertainty satisfy certain integral quadratic inequalities. This allows us to obtain conditions for robust stability that can be expressed as linear matrix inequalities via the Kalman-Yakubovich-Popov lemma.**

***Index Terms*—cross-directional control, robustness, constraints, integral quadratic constraints (IQCs).**

I. Introduction

CROSS-DIRECTIONAL (CD) control is required for many industrial web forming processes (also called sheet and film processes) such as paper making, plastic film extrusion, coating processes and metal rolling. These processes are of great economic importance and hence CD control receives substantial interest from the industrial and academic communities [9]. Improvements in the control of film and sheet processes could mean significant reductions in material equipment, improved product quality, elimination of production waste and reduced energy consumption [34].

The major design challenge for CD controllers does not arise from the dynamic response, but rather comes from the high dimensionality of the multivariable process. This has led to two main design considerations of the controllers: ensuring the control is *robust* [5], [20] to errors in the model, and ensuring the actuators are optimally configured in the presence of *constraints* on the range of their values [21], [2], [29]. Efforts to address the former have led to the decomposition of the process into modes, where the controller is designed to operate only on the reduced (low) modes. If a sufficiently low number of modes is chosen, the actuators will not encounter the constraint boundaries [19] and classical robustness measures can be used [9], [31]. But if the model is well known, increasing the number of modes and dealing explicitly with constraints can improve performance [21], [35]. Although techniques such as Model Predictive Control (MPC) are well suited to this case [28], [12], there are few robustness results that can be usefully applied to such controllers. Interestingly, most of the literature on CD control addresses either robustness or explicit constraint handling but not both simultaneously [6] —e.g. [9].

In [14], the authors propose a novel control design for a particular class of CD processes. In the design, the authors incorporate a nonlinear control law embedded within an Internal Model Control (IMC) structure to achieve optimal constrained steady-state behaviour. Steady-state performance may be improved significantly in some circumstances. Different types of norms may be used for the constrained optimisation performed by the controller. If a 2-norm is used, then the nonlinearity within the control law becomes a Quadratic Program (QP). Such a quadratic program is a continuous sector-bounded nonlinearity (after linear transformation) [15]. In [1], the authors make use of this property to carry out a robust analysis and design for CD control which is limited to a graphical technique: the multivariable circle criterion [18] decomposed according to modes.

Apart from [1], the robustness of cross-directional controllers that handle constraints explicitly is not considered in the literature. This paper proposes a rather more complete robust stability test for the cross-directional design proposed in [14], using the theory of integral quadratic constraints (IQCs) [17], [23]. For the case of diagonal uncertainty, it is shown that the test can be decomposed and hence easily executed on a mode-by-mode form.

The robustness results obtained via IQCs are exploited in the tuning procedure of the controller and combined with a set of heuristic rules. The design methodology extends the performance as much as possible while ensuring closed-loop robustness to plant uncertainties and input static constraints. The proposed design is illustrated in various examples including a simulation case study based on real data from the paperboard industry.

Notation. The treatment in the paper will be developed for discrete-time systems. The symbol l_2 stands for the space of square summable sequences with support on $\mathbb{Z}^+$. The inner product of $x, y \in l_2$ is provided by

$$\langle x, y \rangle = \frac{1}{2\pi} \int_{-\pi}^{\pi} x(e^{j\omega})^* y(e^{j\omega})\, d\omega$$

where $x(e^{j\omega})$ and $y(e^{j\omega})$ denote the Fourier transforms of x and y, respectively.

The norm of a member x of l_2 is induced by its inner product, i.e., $||x|| = \sqrt{\langle x, x \rangle}$. The standard Euclidian norm of

R. M. Morales is with the Control and Instrumentation Research Group, Department of Engineering, University of Leicester, University Road, Leicester, LE1 7RH, UK (e-mail: rmm23@leicester.ac.uk).

W. P. Heath is within Control Systems Centre, School of Electrical and Electronic Engineering, University of Manchester, Sackville Street Building, Manchester, M13 9PL, UK (e-mail: william.heath@manchester.ac.uk).

This work was done while both authors were with the Control Systems Centre, University of Manchester, UK.

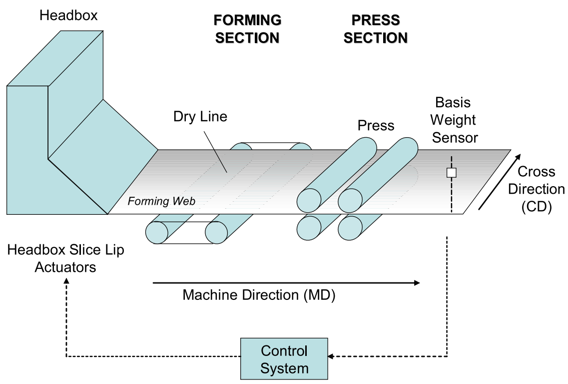

Fig. 1: Simplified schematic of the first stage of a typical paper making process.

a vector x will be denoted by $||x||_2$. The H_∞-norm of a Linear Time-Invariant discrete stable operator $\Delta(z)$ is represented by $||\Delta||_\infty$.

We will also say that an operator $\Delta : x \mapsto \Delta(x)$, acting on the extended space of l_2, is said to satisfy the IQC defined by a measurable and Hermitian-valued function $\Pi(j\omega)$ if

$$\left\langle \begin{bmatrix} x \\ \Delta(x) \end{bmatrix}, \Pi \begin{bmatrix} x \\ \Delta(x) \end{bmatrix} \right\rangle \geq 0, \forall x \in l_2$$

The short-hand notation $\Delta \in \mathrm{IQC}(\Pi)$ will also be used to indicate the above.

Finally, let matrices Π_a and Π_b be structured as

$$\Pi_a = \begin{bmatrix} \Pi_{11}^a & \Pi_{12}^a \\ \Pi_{21}^a & \Pi_{22}^a \end{bmatrix}, \Pi_b = \begin{bmatrix} \Pi_{11}^b & \Pi_{12}^b \\ \Pi_{21}^b & \Pi_{22}^b \end{bmatrix}$$

The diagonal augmentation (daug) operation on Π_a and Π_b is defined as

$$\mathrm{daug}(\Pi_a, \Pi_b) = \begin{bmatrix} \Pi_{11}^a & & \Pi_{12}^a & \\ & \Pi_{11}^b & & \Pi_{12}^b \\ \Pi_{21}^a & & \Pi_{22}^a & \\ & \Pi_{21}^b & & \Pi_{22}^b \end{bmatrix}$$

II. Characteristics of Cross-directional Processes

A. Sheet and Film Processes

Generally, web processes are characterised by the continuous production of a thin web or film in which raw material is continuously (or semi-continuously) fed at the beginning of the production line. A simplified schematic of the initial stage of a typical paper making process is illustrated in Figure 1. The direction in which raw material flows is known as the machine direction (MD). In general, the cross-directional control problem consists in controlling variations in the profile across the strip through actuators and sensor reading positions evenly distributed along the cross-direction (i.e. orthogonal to the MD). For example, in the paper industry, the CD control aims to reduce variations of properties such as basis weight (weight per unit area), moisture content or calliper (thickness) [24]. CD control principles from the paper and plastic industries have also been successfully used in metal strip rolling processes in order to improve the control of the flatness [7]. Overall, there exist different disturbances affecting the process such as variations in the composition of the raw material, uneven distribution of the material in the cross-direction and deviations in the cross-directional profile. In this sense, the CD control system can be thought of as a regulator.

Control actions are effected at a distribution device known as the *headbox* in paper making, and the *die* in coating and polymer extrusion processes [34]. Actuators are almost always evenly spaced across the controlled strip. Sensors operate at a downstream position with respect to the MD and the number of measurements taken by a single scan can be up to 1000. Actuators, which usually vary in number between 30 and 300, are subject to hard physical and bending constraints. Thus, the open-loop process is a large-scale multivariable process.

For more information on the physical description of web forming processes see [9] and the references therein.

B. The Open-loop Model

Generally, each element within the bank of actuators is considered to have the same dynamic response. The open-loop model is used in the control system to represent the effects the actuator actions have on the profile, which are measured by a scanning sensor at n locations evenly spaced across the width of the moving strip. The model used in this work considers only a single measured variable, e.g. basis weight. The nominal open-loop behaviour of the output profile $y(t) \in \mathbb{R}^n$ is usually described by

$$y(t) = h_o(z)Bu(t) + d_o(t) \tag{1}$$

where we define

$$h_o(z) = z^{-k}h(z) \tag{2}$$

The dynamics $h_o(z)$ are represented by a delay of integer k samples z^{-k} and a stable, low order, bi-proper, SISO linear time invariant (LTI) discrete transfer function $h(z)$, with z as the forward shift operator. The delay term z^{-k} is mainly due to the physical separation between the actuators and sensors. In the literature, this model is said to have separable spatial and temporal characteristics and is found in nearly all reported sheet and film processes [9].

Without loss of generality, we assume that $h(1) = 1$ (i.e. $h(z)$ has unit steady state gain). $u(t) \in \mathbb{R}^m$ represents the input or control actions applied to the array of actuators and $B \in \mathbb{R}^{n\times m}$ is called the interaction matrix. The signal $d_o(t) \in \mathbb{R}^n$ is introduced in this model to account for disturbances. Typically $n > m$ with n and m both large positive integers (the number of sensor locations is typically significantly greater then the number of actuators). The singular value decomposition (SVD) of B allows the following factorisation

$$B = \Phi\Sigma\Psi^T \tag{3}$$

where the upper left block of $\Sigma \in \mathbb{R}^{n\times m}$ is a diagonal matrix and $\Phi \in \mathbb{R}^{n\times n}$ and $\Psi \in \mathbb{R}^{m\times m}$. Typically, the interaction matrix B is ill-conditioned, i.e., the ratio between the maximum and minimum singular values is large. This translates in the process having a strong directionality. This is a major consideration in cross-directional processes.

C. Robustness and Modal Decomposition

In reality, it is extremely hard to develop a highly accurate model that describes the open-loop interaction between actuators and sensors across the strip. The plant-model mismatch can be included in the model by uncertainty elements. Sources of uncertainty include the lack of understanding of the underlying phenomena, unmodelled dynamics, unknown disturbances, equipment ageing and the mapping from actuators to sensors.

The open-loop response of web forming processes can be separated into controllable (low) and uncontrollable (high) components via Fourier transforms [3], [30], Gram polynomials [19], [12] or the SVD [9]. This is known as modal decomposition. Usually, the model matches better the real plant at low order modes than at higher ones. Attempts to control ultra high modes may result in closed-loop instability [9], [31]. It is common then that the controller should not act on high-order modes. Following the decision that the controller should only act on r modes, let the SVD of B be further partitioned as

$$B = \begin{bmatrix} \Phi_r & \Phi_\perp & \Phi_0 \end{bmatrix} \begin{bmatrix} \Sigma_r & 0 & 0 \\ 0 & \Sigma_\perp & 0 \\ 0 & 0 & 0 \end{bmatrix} \begin{bmatrix} \Psi_r^T \\ \Psi_\perp^T \\ \Psi_0^T \end{bmatrix} \tag{4}$$

where $\Phi_r \in \mathbb{R}^{n\times r}$ and $\Psi_r \in \mathbb{R}^{m\times r}$ are respectively the first r columns of Φ and Ψ. Note that $r \leq l := \text{rank}(B) \leq \min(m,n)$. Similarly, $\Phi_\perp \in \mathbb{R}^{n\times(l-r)}$, $\Psi_\perp \in \mathbb{R}^{m\times(l-r)}$ and the diagonal matrix $\Sigma_r = \text{diag}(\sigma_1, ..., \sigma_r)$.The matrix factorisation given by (4) can be applied to any $B \in \mathbb{R}^{n\times m}$.

Finally, if the numbers of modes r is sufficiently low, it is possible to design robust controllers which do not violate actuator constraints [8], [9], [19], [20], [31], [5], [16], [33]. Under this strategy, basic IMC-based controllers have also been discussed [3], [9], [19], [32], [29].

D. Actuator Constraints

Constraints on the actuators are usually found in cross-directional control of sheet and film processes because of physical limitations. A class of constraints is known as min-max. This type of constraints restricts actuator movements to a limited range between a maximum and a minimum value. Mathematically, they are expressed as

$$u_{min} \leq u_i(t) \leq u_{max} \tag{5}$$

where $1 \leq i \leq m$. In the case where actuators are steam sprays or heaters used in the paper making industry at the dryer section, excessive actuator set-points may weaken or tear the sheet or film [34].

Some applications of CD control might also require second-order spatial bending constraints

$$\bar{u}_{min} \leq u_{i-1}(t) - 2u_i(t) + u_{i+1}(t) \leq \bar{u}_{max} \tag{6}$$

Constraints of type (6) avoid the amount of “zigzag” among the positions of adjacent actuator. Zigzag constraints might be required in coating processes where adjacent actuators are physically connected to prevent mechanical stresses. Equality constraints are also used sometimes in applications of CD control. For instance, it is helpful to restrict the dimension of the input space [19] by forcing the actuator signals to sum

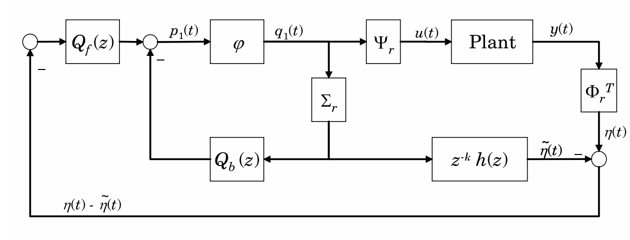

Fig. 2: Cross-directional controller proposed by Heath and Wills.

to zero [14]. All mentioned constraints are time-independent and hence static. Generally, static constraints of any order will be represented by $u(t) \in \mathbb{U}$. Specific static constraints can be highly important for particular sheet and film processes.

Constraints can be explicitly considered in the design of CD controllers. The control law becomes typically a convex optimisation problem such as a quadratic program. Static constraints are usually cast as linear inequalities. The optimisation problem will be computed at each time instance. Modified anti-windup and Model Predictive Control [22] are common approaches for this scenario.

III. The CD Controller of Heath and Wills

Model mismatch at intermediate modes might be relatively small. In such cases heavy restrictions on r (as mentioned in subsection II-C) would result in economic disadvantage [21], [35] at steady state. The final performance can be improved further by increasing r cautiously together with constrained optimisation laws that permit explicit constraint handling [14]. Otherwise if only the number of modes is increased, then the overall control performance might degenerate seriously. Some MPC strategies have been considered for this situation [12], [28]. This work is based on the control structure proposed by [14] for such a possible performance improvement.

This control architecture of [14] is illustrated in Figure 2. It can be understood as a natural generalisation of IMC anti-windup systems for CD processes. It preserves the intuitive-to-tune properties of unconstrained methods whilst ensuring, where possible, optimal steady-state performance. Generally, it allows explicit constraint handling through a constrained optimisation law φ. This CD controller is straightforward for implementation and design where $Q_f(z)$, $Q_b(z)$ and Σ_r are all diagonal.

This controller operates on a limited number of low modes of the process. The decomposition is represented by $q_1(t) \in \mathbb{R}^r$ and $\eta(t) \in \mathbb{R}^r$, which are expressed respectively as

$$q_1(t) = \Psi_r^T u(t) \tag{7}$$

$$\eta(t) = \Phi_r^T y(t) \tag{8}$$

One may interpret (7) as the orthogonal projection of the input signal $u(t)$ on the column space of Ψ_r (col(Ψ_r)). This constitutes an onto transformation because every vector $q_1(t)$ is the image of at least one vector $u(t)$. A similar interpretation can be applied to (8).

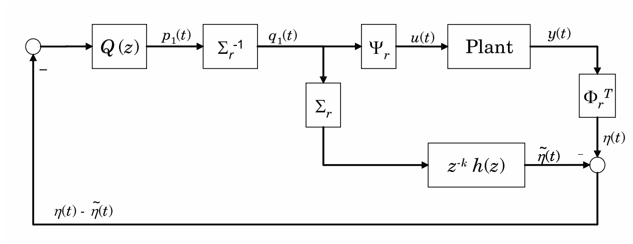

Fig. 3: Control system for unconstrained CD processes.

The equations of the controller are:

$$\begin{aligned} u(t) &= \Psi_r q_1(t) \\ q_1(t) &= \varphi\left(p_1(t)\right) \text{ where } \varphi \text{ is given below} \\ p_1(t) &= Q_f(z)\left(\tilde{\eta}(t) - \eta(t)\right) - Q_b(z)\Sigma_r q_1(t) \\ \tilde{\eta}(t) &= z^{-k}h(z)\Sigma_r q_1(t) \\ \eta(t) &= \Phi_r^T y(t) \end{aligned} \tag{9}$$

The control law $\varphi(\cdot)$ is generally given by

$$\begin{aligned} q_1(t) = \arg\min_{\hat{q}_1(t)} \|\Sigma_r \hat{q}_1(t) - p_1(t)\|_2 \\ \text{such that } \Psi_r \hat{q}_1(t) \in \mathbb{U} \end{aligned} \tag{10}$$

which may also be computed at each time instant as

$$\begin{aligned} q_1(t) = \arg\min_{\hat{q}_1(t)} \frac{1}{2}\hat{q}_1^T(t)\Sigma_r^2\hat{q}_1(t) - \hat{q}_1^T(t)\Sigma_r p_1(t) \\ \text{such that } \Psi_r \hat{q}_1(t) \in \mathbb{U} \end{aligned} \tag{11}$$

In the nominal case this control law achieves optimal steady-state performance with respect to a static disturbance d_o subject to $u(t) \in \mathbb{U}$ and $\Phi_\perp^T u(t) = 0$, [14].

The solution to the optimisation problem (10) when no constraints are imposed is $\varphi = \Sigma_r^{-1}$. This follows because

$$\|\Sigma_r q_1(t) - p_1(t)\|_2 = \|\Sigma_r \Sigma_r^{-1} p_1(t) - p_1(t)\|_2 = 0$$

The control scheme is then represented in this case by Figure 3. The closed-loop response with no model mismatch is

$$y(t) = \left(I - z^{-k}h(z)\Phi_r Q(z)\Phi_r^T\right) d_o(t) \tag{12}$$

The control system is embedded with the IMC anti-windup structure by means of $Q_f(z)$ and $Q_b(z)$ to compensate against input saturations. To preserve standard IMC characteristics when the system operates in the linear (unconstrained) region, the following expression should hold

$$Q(z) = (I + Q_b(z))^{-1} Q_f(z)$$

The diagonal transfer function $Q_f(z)$ is chosen by

$$Q_f(z) = \Lambda Q(z) + (I - \Lambda)Q(\infty) \tag{13}$$

with Λ as a $r \times r$ diagonal matrix whose diagonal elements are scalars denoted by λ_i to trade-off between stability and performance. See [14] and [1] for other choices. It follows then that $Q_b(z)$ should be chosen as

$$Q_b(z) = Q_f(z)Q^{-1}(z) - I \tag{14}$$

Note that $Q_b(z)$ is guaranteed to be strictly proper if $\lambda_i \in [0, 1]$. Also, if $\Lambda = 0$ then $Q_f = Q(\infty)$ becomes constant and this choice has shown to offer good compensation against input saturations [36].

IMC anti-windup has been proved to have good stability properties. If $\Lambda = I$, the system reduces to the conventional IMC structure. Such a choice can preserve the robustness of the unconstrained scenario but the performance be badly deteriorated in the face of input saturations. A rigorous stability analysis of the IMC anti-windup is found in [26].

A. Min-max and second-order bending constraints

The feasibility region is described by a number of one-dimensional linear inequalities. These form a convex region and can also be grouped in a single vector-matrix form [10]. For example, consider actuator min-max and zig-zag constraints, which are given by (5) and (6) respectively. They can be collected by a large linear inequality constraint as follows

$$Au(t) \preceq b$$

where

$$A = \begin{bmatrix} I_{m\times m} \\ -I_{m\times m} \\ \begin{bmatrix} 1 & -2 & 1 & & \\ & 1 & -2 & 1 & \\ & & \ddots & & \\ & & 1 & -2 & 1 \end{bmatrix}_{m\times m} \\ -\begin{bmatrix} 1 & -2 & 1 & & \\ & 1 & -2 & 1 & \\ & & \ddots & & \\ & & 1 & -2 & 1 \end{bmatrix}_{m\times m} \end{bmatrix}$$

and

$$b = \begin{bmatrix} \begin{bmatrix} u_{max} \\ \vdots \\ u_{max} \end{bmatrix}_{m\times 1} \\ -\begin{bmatrix} u_{min} \\ \vdots \\ u_{min} \end{bmatrix}_{m\times 1} \\ \begin{bmatrix} \bar{u}_{max} \\ \vdots \\ \bar{u}_{max} \end{bmatrix}_{m\times 1} \\ -\begin{bmatrix} \bar{u}_{min} \\ \vdots \\ \bar{u}_{min} \end{bmatrix}_{m\times 1} \end{bmatrix}$$

The symbol '$\preceq$' denotes term-by-term inequality. Hence the control law $\varphi(\cdot)$ becomes the following quadratic program

$$\begin{aligned} q_1(t) = \arg\min_{\hat{q}_1(t)} \frac{1}{2}\|\Sigma_r \hat{q}_1(t) - p_1(t)\|_2^2 \\ \text{subject to } A\Psi_r \hat{q}_1(t) \preceq b \end{aligned} \tag{15}$$

B. Performance at the Steady-state

In order to gain insight about the role of the IMC controller $Q(z)$ in the steady-state performance, we investigate the rejection to a time-invariant output disturbance d_o under

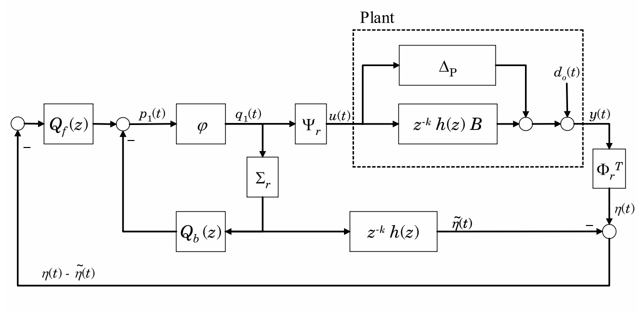

Fig. 4: Closed-loop system for CD processes with modelled uncertainty.

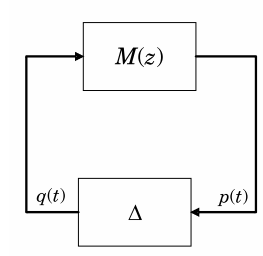

Fig. 5: Standard feedback loop

the conditions of perfect modelling and no constraints, i.e., $\varphi = \Sigma_r^{-1}$. The output profile at steady-state is given by (see (12))

$$y_{ss} = (I - \Phi_r F(1)\Phi_r^T)d_o \tag{16}$$

where $F(z) = h(z)Q(z)$ is a diagonal filter. An indication of the level of disturbance rejection is

$$\|\Phi_r^T y_{ss}\|_2 = \|(I - F(1))\Phi_r^T d_o\|_2$$

It is clear then that the above measure becomes optimal when there is integral action on all modes $F(1) = I$, otherwise the system will attenuate the disturbance up to some extent. The level of rejection is indicated by how close is $F(1)$ to I. Also, y_{ss} can be a useful measure since the steady-state performance of a system driven by the CD controller of [14] can be compared to this output to indicate the achieved level of steady-state performance.

IV. Robust Analysis using IQCs

In order to account for discrepancies between the plant and the model, an uncertainty term $\Delta_P(z) \in \mathbb{C}^{n\times m}$ is introduced in the representation of the process

$$\begin{aligned} P(z) &= z^{-k}h(z)B + \Delta_P(z) \\ y(t) &= P(z)u(t) + d_o(t) \end{aligned} \tag{17}$$

See Figure 4. Assume that the modal decomposition of the plant given by (17) yields

$$\Phi_r^T P(z)\Psi_r = z^{-k}h(z)\Sigma_r + W_L(z)\Delta_r(z)W_R(z) \tag{18}$$

the above follows from

$$P(z) = \Phi(h_o(z)\Sigma + \hat{W}_L(z)\hat{\Delta}_r(z)\hat{W}_R(z))\Psi^T \tag{19}$$

where $\hat{W}_L(z), \hat{\Delta}_r(z)$ and $\hat{W}_R(z)$ are $n \times m$ transfer functions with the upper left block corner as $W_L(z) \in \mathbb{C}^{r\times r}, \Delta_r(z) \in \mathbb{C}^{r\times r}$ and $W_R(z) \in \mathbb{C}^{r\times r}$, respectively, and zeros elsewhere. The weights $W_L(z)$ and $W_R(z)$ are known matrices that characterise the uncertainty in the modal space.

For stability analysis, it is advantageous to express the closed-loop in the feedback configuration depicted in Figure 5. With this aim, define $q_2(t) = \Delta_r(z)q_1(t)$ and $p_2(t) = W_R(z)q_1(t)$. The closed-loop system is completely characterised by

$$\begin{aligned} p(t) &= M(z)q(t) \\ q(t) &= \Delta(p(t)) \end{aligned} \tag{20}$$

where $p(t) = [p_1(t)^T p_2(t)^T]^T$, $q(t) = [q_1(t)^T q_2(t)^T]^T$ and $M(z)$ and Δ are defined as

$$M(z) = \begin{bmatrix} -Q_b(z)\Sigma_r & -Q_f(z)W_L(z) \\ W_R(z) & 0 \end{bmatrix} \tag{21}$$

$$\Delta = \begin{bmatrix} \varphi & 0 \\ 0 & \Delta_r(z) \end{bmatrix} \tag{22}$$

A. Uncertainty in the modal space

In principle, the decomposition in the uncertainty representation in (18) is quite general since it can account for both uncertainty in the dynamics of the process and uncertainty in the modal space of the interaction matrix. Consider for instance the following scenarios:

- Assume $P(z) = (h_o(z) + w(z)\delta(z))B$ with $w(z)$ and $\delta(z)$ being one dimensional elements. The modal decomposition will account for the additive uncertainty in the dynamics of the open-loop process in the modal space, or in other words, *the same* uncertainty in the first r singular values of the interaction matrix. This case is equivalent to assign

$$W_L(z) = \Sigma_r w(z) \tag{23}$$
$$W_R(z) = I \tag{24}$$
$$\Delta_r(z) = \delta(z)I \tag{25}$$

  The discussed uncertainty representation is appropriate for modelling inaccuracies when the sensor is of the tracking-type. All measurements are taken by a single sensor element [9].
- The case where $\Delta_r(z)$ is diagonal accounts for *independent* variations associated to each controlled mode provided the weights $W_L(z)$ and $W_R(z)$ are also diagonal. In this case one of the weights can be set to the identity matrix without loss of generality. A typical assignment for this scenario is

$$W_R(z) = I$$
$$W_L(z) = \begin{bmatrix} w_1(z) & & \\ & \ddots & \\ & & w_r(z) \end{bmatrix}$$

  This representation is more appropriate for representing inaccuracies in the actuator models [4] since each actuator is expected to have somewhat different dynamic response [9].

- If an unstructured $\Delta_r(z)$ is instead considered, then a broader class of uncertainties is taken into account such as changes in the first r subspaces of the column and row spaces of the interaction matrix B and the process dynamics.
- A block-diagonally structured matrix $\Delta_r(z)$ can be used to account for an specific structure in the uncertainty in the modal space.

B. IQCs for the uncertainty Δ_r

In general, we consider Δ_r to be a norm-bounded uncertainty operator. In the IQC framework, such an uncertainty is addressed by saying that $\Delta_r \in \text{IQC}(\Pi_{\Delta_r})$ with

$$\Pi_{\Delta_r} = \begin{bmatrix} \Gamma(j\omega) & 0 \\ 0 & -\Gamma(j\omega) \end{bmatrix} \tag{26}$$

where $\Gamma(j\omega) = \Gamma(j\omega)^* > 0 \, \forall \omega$. This representation corresponds to the description of a whole set of operators from which representative uncertainty sets can be chosen by means of $\Gamma(j\omega)$. We have in particular:

- Let $\Delta_r(z)$ represent a block-diagonally structured LTI uncertainty. An appropriate choice of $\Gamma(j\omega)$ will commute with the uncertainty $\Delta_r(z)$, i.e, ($\Gamma\Delta = \Delta\Gamma$ for all ω). Such a choice is the basis for standard upper bounds of the μ-value [23], [37]. Take for instance
$$\Delta_r(z) = \begin{bmatrix} \delta_1(z) & & \\ & \ddots & \\ & & \delta_r(z) \end{bmatrix}$$
with $\|\delta_i\|_\infty \leq 1$ for all $i = 1...r$. Then
$$\Gamma = \begin{bmatrix} \gamma_1(j\omega) & & \\ & \ddots & \\ & & \gamma_r(j\omega) \end{bmatrix} \tag{27}$$
where $\gamma_i(j\omega)$ is a positive bounded measurable function, see [23].
- If $\Gamma = \gamma(j\omega)I$, with $\gamma(j\omega) > 0 \, \forall \omega$ and a bounded measurable function, then $\Delta_r(z)$ corresponds to a LTI unstructured norm-bounded operator with $||\Delta||_\infty \leq 1$ [23].
- If $\Gamma = \gamma I$, where $\gamma > 0$ and constant, then Δ_r corresponds to a broader class of uncertainty operators with bounded gain [23]. Note that Δ_r is not longer restricted to be a LTI operator for such a choice of Γ.

For other types of operators to express uncertainty under the IQC terminology refer to [23].

C. QP as a Sector-bounded Nonlinearity

The QP in (15) satisfy an important integral quadratic constraint which is used in the stability analysis. Using IQC notation, it can be stated that solutions of the QP in (15) satisfy the following condition

$$\left\langle \begin{bmatrix} p_1 \\ q_1 \end{bmatrix}, \Pi_\varphi \begin{bmatrix} p_1 \\ q_1 \end{bmatrix} \right\rangle \geq 0 \tag{28}$$

with

$$\Pi_\varphi = \begin{bmatrix} 0 & \Sigma_r \\ \Sigma_r & -2\Sigma_r^2 \end{bmatrix}$$

For more information refer to [15], [13].

D. IQCs for Combined Uncertainty and Nonlinearity Δ

The operator Δ, defined in (22), satisfy the IQC condition defined by

$$\Pi_\Delta = \text{daug}(\Pi_\varphi, \Pi_{\Delta_r}) = \begin{bmatrix} \Pi_{\Delta(11)} & \Pi_{\Delta(12)} \\ \Pi_{\Delta(21)} & \Pi_{\Delta(22)} \end{bmatrix}$$

where

$$\Pi_{\Delta(11)} = \begin{bmatrix} 0 & \\ & \Gamma \end{bmatrix}$$
$$\Pi_{\Delta(22)} = \begin{bmatrix} -2\Sigma_r^2 & \\ & -\Gamma \end{bmatrix}$$
$$\Pi_{\Delta(12)} = \Pi_{\Delta(21)} = \begin{bmatrix} \Sigma_r & \\ & 0 \end{bmatrix}$$

Since $\Pi_{\Delta(11)} \geq 0$ and $\Pi_{\Delta(22)} \leq 0$ then the following statement holds [17]

$$\Delta \in \text{IQC}(\Pi_\Delta) \Rightarrow \; \tau\Delta \in \text{IQC}(\Pi_\Delta) \qquad \forall \, \tau \in [0,1] \tag{29}$$

E. Stability Criterion

The following result is a direct application of the main IQC theorem [23].

Result 1. The system (20) with controller (11) is stable provided

$$\begin{bmatrix} M(e^{j\omega}) \\ I \end{bmatrix}^* \Pi_\Delta \begin{bmatrix} M(e^{j\omega}) \\ I \end{bmatrix} \leq -\varepsilon I \tag{30}$$

for some $\varepsilon > 0$, for all $\omega \in [-\pi, \pi]$ and where M is given by (21). $\square$

Stability is claimed in the input-output sense of [23] and [17]. Statement (29), which has been shown to hold here, is a necessary condition of the main IQC theorem. In addition, if $M(z)$ has the following state-space representation

$$\begin{bmatrix} A_M & B_M \\ C_M & D_M \end{bmatrix} \sim M(z) = C_M(zI - A_M)^{-1}B_M + D_M$$

where the pair (A_M, B_M) is controllable and A_M has no eigenvalues on the imaginary axis (det$(e^{j\omega}I - A_M) \neq 0$), then the stability condition (30) may be rewritten as

$$\begin{bmatrix} (e^{j\omega}I - A_M)^{-1}B_M \\ I \end{bmatrix}^* \Pi \begin{bmatrix} (e^{j\omega}I - A_M)^{-1}B_M \\ I \end{bmatrix} \leq -\varepsilon I \tag{31}$$

where Π is structured as

$$\Pi = \begin{bmatrix} \Pi_{11} & \Pi_{12} \\ \Pi_{21} & \Pi_{22} \end{bmatrix}$$

with

$$\begin{aligned} \Pi_{11} &= C_M^T \Pi_{\Delta(11)} C_M \\ \Pi_{12} &= \Pi_{21}^* = C_M^T \Pi_{\Delta(12)} + C_M^T \Pi_{\Delta(11)} D_M \\ \Pi_{22} &= \Pi_{\Delta(22)} + \Pi_{\Delta(21)} D_M + D_M^T \Pi_{\Delta(12)} \\ & \quad + D_M^T \Pi_{\Delta(11)} D_M \end{aligned} \tag{32}$$

Via the discrete-time Kalman-Yakubovich-Popov (KYP) lemma [27], inequality (31) is satisfied if and only if there exists some matrix $P^T = P$ such that

$$\begin{bmatrix} A_M^T P A_M - P & A_M^T P B_M \\ B_M^T P A_M & B_M^T P B_M \end{bmatrix} + \Pi \leq 0$$

V. Decomposition

In the previous section a sufficient condition for robust stability has been derived in terms of a large scale Linear Matrix Inequality (LMI). In certain cases it is possible to decompose the result and test each mode in turn. The decomposition of the frequency-domain test facilitates the computational task because the dimensions of the treated matrices can be significantly lower. Computations with large dimensional matrices could lead to numerical problems and/or larger computational times.

A. Diagonal Uncertainty

Assume that uncertainty $\Delta_r(z)$ is diagonal so Γ is given by equation (27). Assume further that the weights $W_L(z)$ and $W_R(z)$ are diagonal: $W_R(z) = \text{diag}(w_{R1}(z), ..., w_{Rr}(z))$ and $W_L(z) = \text{diag}(w_{L1}(z), ..., w_{Lr}(z))$. It follows from (30) that if there exists a $\Gamma > 0$ and $\epsilon > 0$ such that

$$\begin{bmatrix} -\Sigma_r^2(Q_b^* + Q_b + 2I) + \Gamma W_R^* W_R & -\Sigma_r Q_f W_L \\ -W_L^* Q_f^* \Sigma_r & -\Gamma \end{bmatrix} \leq -\varepsilon I \tag{33}$$

$\forall\omega \in [-\pi, \pi]$, then the system (20) is guaranteed stable. This stability condition might also be expressed as follows.

Result 2. The inequality (33) is true if and only if

$$\begin{bmatrix} -\sigma_i^2(q_{bi}^* + q_{bi} + 2) + \gamma_i|w_{Ri}|^2 & -\sigma_i q_{fi} w_{Li} \\ -\sigma_i w_{Li}^* q_{fi}^* & -\gamma_i \end{bmatrix} \leq -\varepsilon I \tag{34}$$

for $i = 1, \ldots, r$, where q_{fi} and q_{bi} are the ith diagonal entries of Q_f and Q_b respectively. The arguments $(e^{j\omega})$ have been omitted for conciseness.
Proof. Suppose $e = [e_1, e_2]$ is an eigenvector of the matrix on the left hand side of (34) with eigenvalue λ for some i and at some frequency ω. Define the vector $\bar{e} \in \mathbb{R}^{2r\times 1}$ to have all zero entries except $\bar{e}_i = e_1$ and $\bar{e}_{r+i} = e_2$. Then $\bar{e}$ is an eigenvector of the matrix on the left hand side of (33) with eigenvalue λ. $\square$

Note that the condition in Result 2 at each frequency can be reduced to a LMI feasibility problem in the variable γ_i. The condition however can be further simplified such that the term γ_i does not appear in the condition.
Result 3. Condition (34) holds if and only if

$$\frac{|q_{fi} w_{Li} w_{Ri}|}{\sigma_i} \leq \text{Re}\{q_{bi} + 1\}, \forall\omega \tag{35}$$

Proof. Define

$$b := 2\frac{\text{Re}\{q_{bi} + 1\}\sigma_i^2}{|w_{Ri}|^2}$$

$$c := \frac{|\sigma_i q_{fi} w_{Li}|}{|w_{Ri}|}$$

Condition (34) is satisfied if and only if

$$f(\gamma_i) := (\gamma_i - \hat{\gamma}_1)(\gamma_i - \hat{\gamma}_2) < 0 \tag{36}$$

for any $0 < \gamma_i < b$ where

$$\hat{\gamma}_2 = \frac{b}{2} + \frac{\sqrt{b^2 - 4c^2}}{2} \tag{37}$$

$$\hat{\gamma}_1 = \frac{b}{2} - \frac{\sqrt{b^2 - 4c^2}}{2} \tag{38}$$

We will show that $b \geq 2c$ is a necessary and sufficient condition of (36). For sufficiency, note that if $b \geq 2c$ then condition (36) is satisfied for any $\gamma_i \in (\hat{\gamma}_1, \hat{\gamma}_2)$. For necessity, assume that $0 < b < 2c$ then

$$f(\gamma_i) = \left(\gamma_i - \frac{b}{2}\right)^2 + \left(c^2 - \frac{b^2}{4}\right) > 0 \tag{39}$$

for any γ_i. $\square$

In this scenario the stability test has been *fully* decomposed and the computational task eased. Should the robustness be tested against a wider class of norm-bounded uncertainty δ_i, i.e, a fixed γ_i, then in addition to the condition in Result 3, it is required that

$$\max_{\omega} \hat{\gamma}_1(\omega) < \min_{\omega} \hat{\gamma}_2(\omega), \ \forall\omega \tag{40}$$

A similar discussion is developed for the robustness of the anti-windup IMC structure in [25].

B. Partially decoupled stability test

Result 1 does not apply solely to diagonally-structured uncertainty, it can also apply to unstructured uncertainty $\|\Delta_r\|_\infty \leq 1$ since $\Gamma = \gamma(j\omega)I$ with $\gamma(j\omega) > 0, \forall\omega$. Provided both uncertainty weights $W_L(z)$ and $W_R(z)$ are diagonal, the stability test is then *partially* decomposed

$$\begin{bmatrix} -\sigma_i^2(q_{bi}^* + q_{bi} + 2) + \gamma|w_{Ri}|^2 & -\sigma_i q_{fi} w_{Li} \\ -\sigma_i w_{Li}^* q_{fi}^* & -\gamma \end{bmatrix} \leq -\varepsilon I \tag{41}$$

This frequency-domain criterion differs from (34) in the form it is executed. Stability (41) has to be satisfied with a unique $\gamma(j\omega)$ for all modes whereas (34) allows a different γ_i for every mode.

VI. Controller Tuning

In the cross-directional control field it is usually assumed the open-loop dynamics are described by a first-order transfer function plus some time delay.

$$h_o(z) = z^{-k}\left(\frac{1-a}{1-az^{-1}}\right)c_h \tag{42}$$

Under this scenario, algorithms for tuning the controllers $Q_f(z)$ and $Q_b(z)$ are developed. The strategy exploits the robustness criteria given in section V and follow the tuning rules proposed in [1]. The above model with unity dc gain ($c_h = 1$) is similar to that used in the simulations performed by [14] and [1].

Standard IMC procedures for the plant model in (42) gives a $Q(z)$ with diagonal elements as

$$q_i(z) = \left(\frac{1-b_i}{1-b_i z^{-1}}\right)\left(\frac{1-az^{-1}}{1-a}\right)\mu_i/c_h \tag{43}$$

The parameters b_i and $\mu_i < 1$ are adjusted to modify the closed-loop bandwidth and the integral action on the corresponding mode.

The elements $Q_f(z)$ and $Q_b(z)$ are obtained by means of (13) and (14) and they are included to compensate against the input constraints. Further trade-off between robustness and performance is provided through Λ which account for the level of anti-windup. Overall, the tuning problem for the CD controller of [14] consists in developing tuning rules for the parameters b_i, μ_i and λ_i.

The controller parameters b_i, μ_i and λ_i are proposed to be chosen as follows:

- b_i should take as small as possible a value in the range $[b_{min}, b_{max}]$, where $0 \leq b_{min} < b_{max} < 1$. The lower b_i the faster this mode acts (better time-domain performance).
- $b_{i+1} \geq b_i$. This is enforced since the level of uncertainty for mode i is less than mode $i+1$.
- μ_i should be chosen as near to 1 as possible. This was discussed in section III-B. Low values of μ_i will deteriorate the steady-state performance. No integral action is expected to happen at the last few modes where the relative model mismatch is greater and hence integral action becomes undesirable [31].
- At low modes $\lambda_i = 0$ so that $q_{fi}(z) = q_i(\infty)$, i.e, the strongest form of anti-windup is imposed at the low modes where integral action is expected to happen.

Controllers with parameters designed in this manner are straightforward to implement [14], [1]. Their benefits over unconstrained design depend on the relative plant uncertainty and the relative size of the actuator constraints [21], [35].

The afore-mentioned heuristics are combined with the robustness criteria previously obtained in order to provide the best possible performance while ensuring stability against the given plant uncertainty and static actuator constraints. The algorithms begin with the most aggressive controller (fastest response, optimal steady-state performance and full anti-windup) and then test if the resulting closed-loop is guaranteed stable. If it is not successful, then the controller is gradually detuned until the stability criteria is satisfied.

The first algorithm displayed in Figure 6 handles the general stability criteria expressed in Result 1. Under ideal conditions, the best performance would be obtained with a fast controller ($b_i = b_{min}$), integral action ($\mu_i = 1$) and full anti-windup ($\lambda_i = 0$) on all modes ($i = 1...r$ with $r = m$). This controller is not expected to guarantee robustness mainly because large control actions would be required to drive the last modes and this could lead to instability. Hence the search for a robust controller may be narrowed down by reducing the initial dimension of the controller $r < m$. The algorithm then proceeds to detune the controller and stops the search once the robustness condition is met. The stability test might be performed in the frequency domain or as an LMI via the KYP lemma (31). Should a robust controller be found once the algorithm is executed, its dimension is indicated by the final value of r and should be independent from the initialisation of r.

The second algorithm, illustrated in Figure 7, exploits the decomposed stability criteria given in section V and simplifies greatly the synthesis task from a computational point of view. This algorithm is performed on a mode-by-mode basis. Unlike the first algorithm, the search in this case is not stopped as soon the stability criterion is satisfied. Instead, it stops after the most robust controller (no anti-windup $\lambda_i = 1$, slow response $b_i = b_{max}$ and no integral action $\mu = \mu_{min}$) is tried at mode i. Of course, if this controller does not guarantee robustness even for the first mode, then a robust controller is not obtained under this strategy. The dimension of the obtained robust controller is given by $i - 1$ after the algorithm is executed.

The above algorithms assume that b_i, μ_i and λ_i are incremented or reduced accordingly until they hit exactly their limit values. In other words, it is assumed that $(b_{max} - b_{min})/\Delta_b$, $(1-\mu_{min})/\Delta_\mu$ and $1/\Delta_\lambda$ are positive integers. The operation enclosed by a dashed-lined box resets the value of μ_i to 1 because μ_i should be as close as possible to 1. Both algorithms guarantee that $b_i \leq b_{i+1}$ and this condition reduces the number of computations.

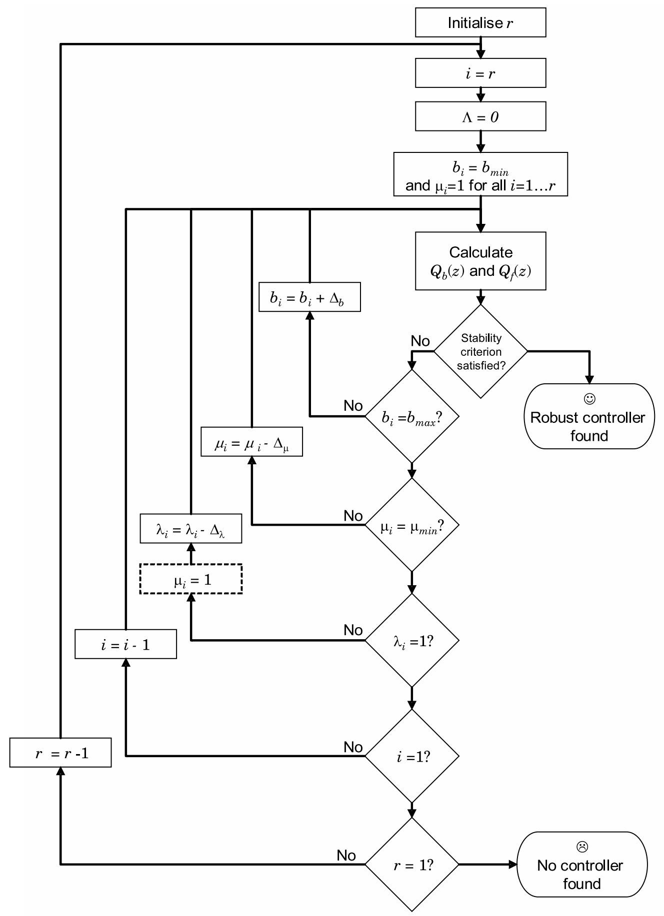

Fig. 6: Tuning algorithm for non-diagonal uncertainties

VII. A Case Study from the Paperboard Machine Industry

Delay (sec)	**Gain**	**Time constant** (sec)
205	-0.107	50
193.6	-0.082	45
200	-0.11	41.9
190	-0.12	35

TABLE I: Real variations in the dynamics of a open-loop process in the paper machine industry. Courtesy of Iggesund Paperboard Ltd.

This section presents a design procedure of a robust CD controller in the paperboard industry. The variations in the dynamics of a real open-loop process have been supplied by

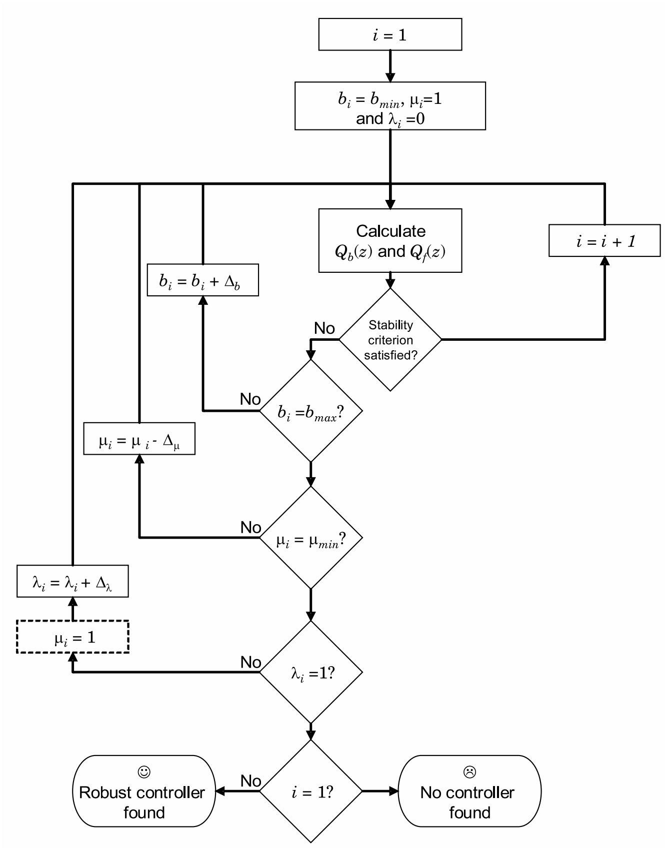

Fig. 7: Tuning algorithm for diagonal uncertainties.

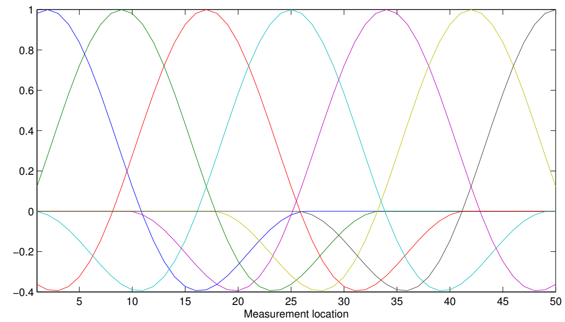

Fig. 8: The steady-state response of a step change in actuators $u_i = 1$ $(i = 1, 5, 10, ..., 30)$ on downstream profile measurement.

Iggesund Paperboard Ltd. Initial data provides time-domain specifications of the mapping between the CD actuators and the scanned profiles from a series of bump tests, see Table I. The measurements were carried out for the production of a paperboard strip with basis weight 100 g/m^2 and calliper of 540 microns. The weight process is controlled by means of dilution actuators at the headbox. Actuator units are fibre to water ratio, normally about 2% fibre and 98% water.

The data was obtained by the identification tool IntelliMap [11] developed to provide an industrial-quality automated identification of CD processes including time response, alignment, shrinkage and CD response shapes.

The open loop behaviour is represented by a single (uncertain) transfer function and a typical interaction matrix B which is shown in Figure 8. The discrete nominal model might then be represented by equation (42). The interaction matrix B has dimension 50×30, that is, the process has 30 actuators and 50 sensor scanning positions in the CD. We now proceed to develop a suitable uncertainty model.

A. Uncertainty Modelling and Controller tuning

The continuous transfer function that describes first-order dynamics plus a time delay is described by

$$\begin{aligned} h_o(s) &= e^{-sk_c} h(s) \\ h(s) &= \frac{1/\tau}{s + 1/\tau} c_h \end{aligned} \tag{44}$$

where k_c, c_h and τ denote the delay, gain and time constant respectively. The information on the variation of the parameters is summarised as follows

$$\begin{aligned} 190 \le k_c \le 205 \\ 35 \le \tau \le 50 \\ -0.12 \le c_h \le -0.082 \end{aligned}$$

The discretisation of the continuous model $h_o(s)$, done with a sampling time T using the step invariance method, provides

$$h_o(z) = z^{-(k_c/T)} \left(\frac{1 - e^{-T/\tau}}{1 - e^{-T/\tau} z^{-1}} \right) c_h \tag{45}$$

where the ratio k_c/T must be an integer. The model (45) is described as (42) provided

$$\begin{aligned} a &= e^{-T/\tau} \\ k &= \frac{k_c}{T} \end{aligned}$$

Also, $Q(\infty)$ is given with its diagonal elements as

$$q_i(\infty) = \frac{\mu_i(1 - b_i)}{c_h(1 - a)} \tag{46}$$

Throughout the simulations, the sampling period is $T = 30$ seconds.

The uncertainty in the dynamics of the process are encapsulated by an additive form

$$\tilde{h}(z) = h_o(z) + w(z)\delta(z) \tag{47}$$

with $\|\delta\|_\infty < 1$. From a practical point of view, the controller is designed to ensure robustness against the wider set of uncertainty given by a constant and positive γ, that is, when Δ_r is a norm-bounded operator (not only unstructured and LTI). This uncertainty assumption accounts for both dynamic uncertainty and some variations in the modal space of the interaction matrix. The stability test become partially decoupled bringing benefits by reducing the computational load of the tuning algorithms. The weights of the uncertainty description $W_L(z)$ and $W_R(z)$ are taken as (23) and (24), respectively.

For the studied case, the parameters of the nominal model – a first order discrete transfer function plus time delay – are chosen as the average of their values

$$h_o(z) = z^{-7} \left(\frac{0.5025}{1 - 0.4975z^{-1}} \right) (-0.1047) \tag{48}$$

Since

$$|\tilde{h}(e^{j\omega}) - h_o(e^{j\omega})| = |w(e^{j\omega})\delta(e^{j\omega})| \le |w(e^{j\omega})| \tag{49}$$

$\forall \omega \in [-\pi, \pi]$, the dynamics weight $w(z)$

$$w(z) = \frac{0.075629(z - 0.8411)(z - 0.7092)}{z^2 - 1.259z + 0.4052} \tag{50}$$

is found by fitting the upper-bound of the magnitude error of every variation of the real process and the nominal transfer function, see Figure 9.

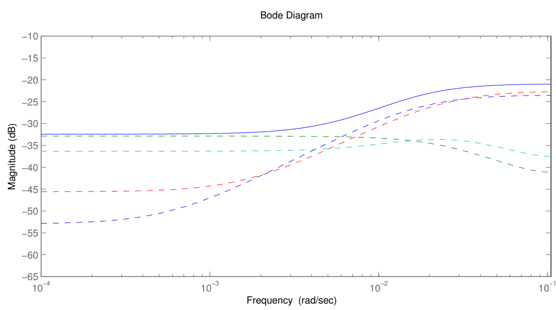

Fig. 9: Second-order uncertainty weight $w(z)$ (solid line) and magnitude of the error between variations of the real process and the nominal transfer function (dashed line).

The tuning of the controller was done by means of the algorithm proposed for scenarios in which the stability criterion is either partially or fully decomposed. In particular, the algorithm executes the test (41) for a fixed value of γ. If possible, the algorithm returns controllers $Q_f(z)$ and $Q_b(z)$ which follow rules (13) and (14), respectively. In addition, an iteration over the γ is carried out until a satisfactory performance is achieved. In the end, it was obtained that with a value of $\gamma = 1$, control can be performed until mode $r = 7$. Parameter values of the designed controller are shown in Figure 10. The obtained controller offers a rather small bandwidth ($0.909 \le b_i \le 0.999$). Integral action is taken on most of the controlled modes and they are accompanied by strong levels of anti-windup which will improve performance in the face of input saturations. The controller is further detuned for the benefit of robustness in the last mode in terms of the parameter λ_i.

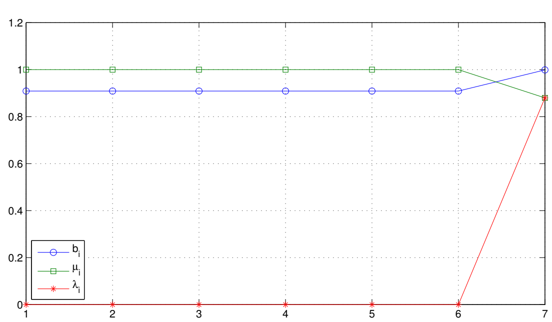

Fig. 10: Tuning parameters b_i, μ_i and λ_i. Control is effected up to mode 16.

B. Simulation Results

The dynamics of the real plant are assumed to be the following discrete model

$$\tilde{h}(z) = (-0.12)\frac{0.5756}{1 - 0.4244z^{-1}} \quad z^{-7}$$

The step response of the plant provides first order dynamics with a steady-state value of -0.12, a delay of 210 seconds and a time constant of 35 seconds.

The speed of the disturbance rejection can be observed from the output $y(t)$ depicted in Figure 11(a). The steady-state output value is displayed in Figure 11(b) and compared against the static disturbance d_o. Also, observe that the level of rejection to the disturbance is similar to the ideal scenario of no constraints and perfect modelling. Overall, it can be said that the designed controller yields an acceptable output disturbance rejection (in terms of both speed and final attenuation) and also ensures robustness against plant uncertainty and input constraints. The control signals shown in Figure 12 do not violate min-max constraints ($u_{max} = -u_{min} = 0.018$) and zigzag constraints ($\bar{u}_{max} = -\bar{u}_{min} = 0.01$). The simulation runs up to discrete time $t = 100$, i.e., 3000 seconds.

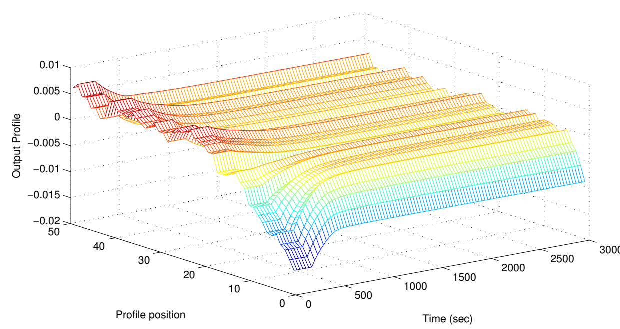

(a) Output profile $y(t)$

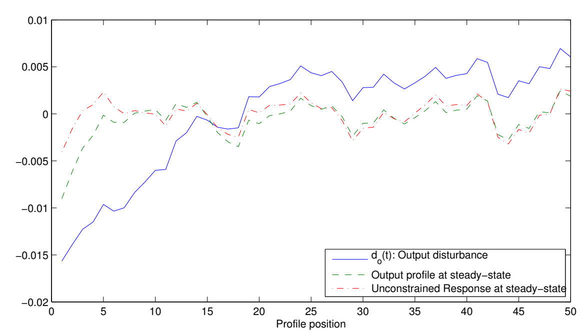

(b) Steady-state Performance

Fig. 11: Output profile $y(t)$ and steady-state performance

VIII. Conclusions

A new robust stability test for constrained cross-directional control has been obtained by means of the theory of IQCs. The test can be expressed in terms of an LMI, and allows analytic expressions for uncertainty sets. Under the assumption that the uncertainty is diagonal in the mode space, the test may be fully decomposed. With an unstructured uncertainty model, the test become partially decomposed—suboptimal

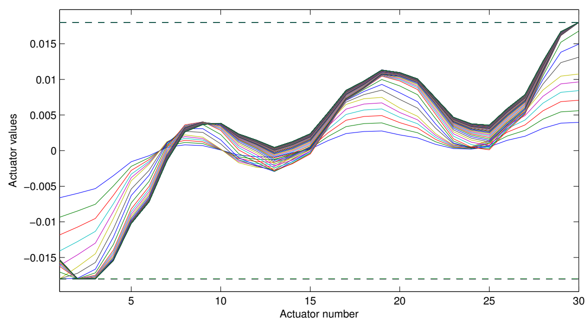

(a) Min-max constraints

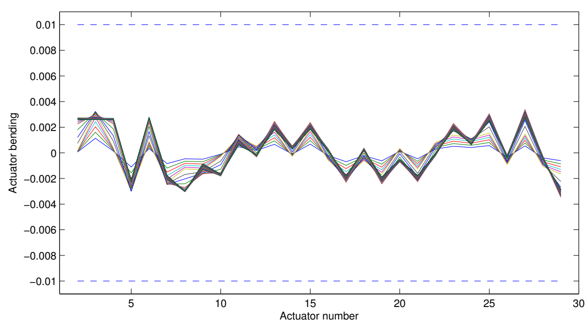

(b) Zigzag constraints

Fig. 12: Control signals $u(t)$

tests may be performed on a mode by mode basis, with a single (scalar) multiplier linking the separate modes. Such decompositions bring benefits in the computer implementation of the robustness criteria.

In addition, the paper exploits the stability test for the tuning of a class of CD controllers to ensure robustness against plant uncertainty and input constraints. One of the developed tuning algorithms was applied to a case study from the paperboard industry. The controller was designed and tuned to achieve acceptable levels of performance while ensuring robustness for large plant variations and static input constraints. The tuning techniques are easy to implement and are based on the appealing features of the IMC methodology.

Acknowledgements

The authors would like to thank Iggensund Paperboard Ltd., in particular Matthew Taylor, for providing data used in this work.

References

[1] J. A. G. Akkermans, W. P. Heath, and A. G. Wills. Robust cross-directional control of paper making machines with saturating acutators. Québec, Canada, 2004. PAPTAC Control Systems 2004.

[2] R. D. Braatz, M. L. Tyler, M. Morari, F. R. Pranckh, and L. Sartor. Identification and cross-directional control of coating processes. *AIChE*, 38:1329 – 1339, 1992.

[3] S. R. Duncan. *The cross-directional control of web-forming processes*. PhD thesis, University of London, 1989.

[4] S. R. Duncan. The design of robust cross-directional control systems for paper making. Technical Report 807, Control Systems Centre, UMIST, 1994.

[5] S. R. Duncan. The design of robust cross-directional control system for paper making. Seattle, USA, 1995. Proceedings of the American Control Conference.

[6] S. R. Duncan. Editorial - special section: Cross directional control. *IEE Proc.-Control Theory Appl.*, 149(5):412–413, 2002.

[7] S. R. Duncan, J. R. Allwood, and S. S. Garimella. The analysis and design of spatial control systems in strip metal rolling. *IEEE Transactions on Control Systems Technology*, 6(2):220–232, 1998.

[8] S. R. Duncan and G.F. Bryant. The spatial bandwidth of cross-directional control systems for web processes. *Automatica*, 33(2):139–153, 1997.

[9] A. P. Featherstone, J. G. VanAntwerp, and R. D. Braatz. *Identification and Control of Sheet and Film Processes*. Springer-Verlag, London, 2000.

[10] R. Fletcher. *Practical Methods of Optimization (second edition)*. John Wiley & Sons, 1987.

[11] D. M. Gorinevski and Gheorghe C. Identification tool for cross-directional processes. *IEEE Transactions on Control Systems Technology*, 11(5):629–640, 2003.

[12] W. P. Heath. Orthogonal functions for cross-directional control of web forming processes. *Automatica*, 32(2):183–198, 1996.

[13] W. P. Heath. Multipliers for quadratic programming with box constraints. Grenoble, France, 2006. Proceedings of the IFAC Workshop on Nonlinear Model Predictive Control for Fast Systems.

[14] W. P. Heath and A. G. Wills. Design of cross-directional controllers with optimal steady state performance. *European Journal of Control*, 10:15–27, 2004.

[15] W. P. Heath, A. G. Wills, and J. A. G. Akkermans. A suficient condition for the stability of optimizing controllers with saturating actuators. *International Journal of Robust and Nonlinear Control*, 15:515–529, 2005.

[16] M. Hovd, R. D. Braatz, and S. Skogestad. Svd controllers for H_2, H_∞ and μ-optimal cotrol. Piscataway, USA, 1994. Proceedings of the American Control Conference.

[17] U. Jönsson. Lecture notes on integral quadratic constraints. Department of Mathematics, KTH, Stockholm. ISBN 1401-2294, available at http://www.math.kth.se/˜uj/, 2000.

[18] H. K. Khalil. *Nonlinear Systems (third edition)*. Prentice Hall, Upper Saddle River, 2002.

[19] K. Kristinsson and G. A. Dumont. Cross directional control on paper machines using gram polynomials. *Automatica*, 32:533–548, 1996.

[20] D. L. Laughlin, M. Morari, and R. D. Braatz. Robust performance of cross-directional basis weight control in paper machines. *Automatica*, 29(6):1395–1410, 1993.

[21] D. L. Ma, J. G. VanAntwerp, M. Hovd, and R. D. Braatz. Quantifying the potential benefits of constrained control for a large-scale system. *IEE Proc.-Control Theory Appl.*, 149(5):423–432, 2002.

[22] J. M. Maciejowski. *Predictive Control with Constraints*. Prentice Hall, 2001.

[23] A. Megretski and A. Rantzer. System analysis via integral quadratic constraints. *IEEE Transactions on Automatic Control*, 42(6):819–830, 1997.

[24] S. Mijanovic. *Paper machine cross-directional control near spatial domain boundaries*. PhD thesis, The University of British Columbia, 2004.

[25] R. M. Morales, W. P. Heath, and G. Li. Robust anti-windup against LTI structured uncertainty using frequency depedent IQCs. Fukuoka, Japan, 2009. Proceedings of the ICCAS-SICE 2009 Conference.

[26] R. M. Morales, G. Li, and W. P. Heath. Anti-windup and the preservation of robusntess against structured norm-bounded uncertainty. Seoul, Korea, 2008. IFAC World congress.

[27] A. Rantzer. On the Kalman-Yakubovich-Popov lemma. *Systems and Control Letters*, 28:7–10, 1996.

[28] J. B. Rawlings and I.-L. Chien. Gage control of film and sheet-forming processes. *AIChE Journal*, 42:753–766, 1996.

[29] O. J. Rojas, G. C. Goodwin, and G. V. Johnston. A spatial frequency anti-windup strategy for cross-directional control problems. *IEE Proc.-Control Theory Appl.*, 149(5):414 – 422, 2002.

[30] G. E. Stewart. *Two dimensional loop shaping controller design for paper machine cross-directional processes*. PhD thesis, The University of British Columbia, 2000.

[31] G. E. Stewart, D. M. Gorinevsky, and G. A. Dumont. Two-dimensional loop shaping. *Automatica*, 39:779–792, 2003.

[32] J. G. VanAntwerp and R. D. Braatz. Robust control of large scale paper machines. Dallas, USA, 1999. AIChE annual meeting.

[33] J. G. VanAntwerp, A. P. Featherstone, and R. D. Braatz. Robust cross-directional control of large scale sheet and film processes. *Journal of Process Control*, 11:149–178, 2001.

[34] J. G. VanAntwerp, A. P. Featherstone, R. D. Braatz, and B. A. Ogunnaike. Cross-directional control of sheet and film processes. *Automatica*, 43:191–211, 2007.

[35] A. G. Wills and W. P. Heath. Analysis of steady-state performance for cross-directional control. *IEE Proc.-Control Theory Appl.*, 149(5):433–440, 2002.

[36] A. Zheng, M. V. Kothare, and M. Morari. Anti-windup design for internal model control. *International Journal of Control*, 60(5):1015–1024, 1994.

[37] K. Zhou and J. C. Doyle. *Essentials of Robust Control*. Prentice Hall, 1998.